IOPscience iopscience.iop.org

Home Search Collections Journals About Contact us My IOPscience

Statistical properties of two-particle transmission at an Anderson transition

This article has been downloaded from IOPscience. Please scroll down to see the full text article.

2009 J. Phys. A: Math. Theor. 42 475007

(http://iopscience.iop.org/1751-8121/42/47/475007)

View the table of contents for this issue, or go to the journal homepage for more

Download details:
IP Address: 171.66.16.156
The article was downloaded on 03/06/2010 at 08:23

Please note that terms and conditions apply.

J. Phys. A: Math. Theor. **42** (2009) 475007 (10pp) doi:10.1088/1751-8113/42/47/475007

Statistical properties of two-particle transmission at an Anderson transition

Cécile Monthus and Thomas Garel

Institut de Physique Théorique, CNRS and CEA Saclay 91191 Gif-sur-Yvette Cedex, France

E-mail: cecile.monthus@cea.fr

Received 11 September 2009, in final form 14 October 2009
Published 9 November 2009
Online at stacks.iop.org/JPhysA/42/475007

Abstract

The ensemble of $L \times L$ power-law random banded matrices, where the random hopping $H_{i,j}$ decays as a power-law $(b/|i-j|)^a$, is known to present an Anderson localization transition at $a = 1$, where one-particle eigenfunctions are multifractal. Here we study numerically, at this critical point, the statistical properties of the transmission T_2 for two distinguishable particles, two bosons or two fermions, in the non-interacting case. We find that the statistics of T_2 is multifractal, i.e. the probability to have $T_2(L) \sim 1/L^{\kappa}$ behaves as $L^{\Phi_2(\kappa)}$, where the multifractal spectrum $\Phi_2(\kappa)$ for fermions is different from the common multifractal spectrum concerning distinguishable particles and bosons. However, in the three cases, the typical transmission $T_2^{\rm typ}(L)$ is governed by the same exponent $\kappa_2^{\rm typ}$, which is much smaller than the naive expectation $2\kappa_1^{\rm typ}$, where $\kappa_1^{\rm typ}$ is the typical exponent of the one-particle transmission $T_1(L)$.

PACS numbers: 71.30.+h, 72.15.Rn, 05.45.Df

(Some figures in this article are in colour only in the electronic version)

1. Introduction

Whereas Anderson localization phenomena [1] are quite well understood for a single particle (see the reviews [2–4]), the case of interacting particles in a random potential has remained much more challenging (see the review [5] and more recent works [6–11]). Since the case of a finite density of particles can be studied numerically only for small system sizes, it is natural to consider first the simpler case of only two interacting particles (TIP) in a random potential. In dimension $d = 1$, where the one-particle model is always in the localized phase with some localization length λ_1, it has been found that the TIP model is also always localized, but with a localization length λ_2 that may become much larger than λ_1 [12–21]. In dimension $d = 2$, where the one-particle model is again always in the localized phase, the possibility of

 © 2009 IOP Publishing Ltd Printed in the UK

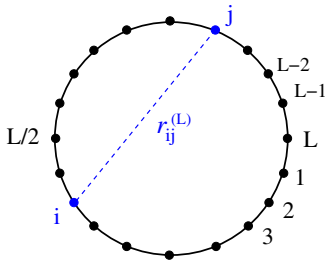

Figure 1. The ensemble of power-law random banded matrices of size $L \times L$ can be represented as a ring of L sites, where the matrix element $H_{i,j}$ between the sites i and j is a Gaussian variable of zero-mean $\overline{H_{i,j}} = 0$ and of variance given by equation (2) in terms of the distance $r_{i,j}$ of equation (1).

a delocalization transition has been studied for short-range interaction [22] and for Coulomb interaction [23–25].

In the present paper, we are interested in the two-particle transport properties at the Anderson localization transition of the one-particle problem, where the one-particle eigenstates are multifractal [2, 4]. We are not aware of the previous studies on this question (see however [26] concerning the quasi-periodic Aubry–André transition). Since for the tight-binding model in dimension $d = 3$, where there exists an Anderson transition, the two-particle model cannot be studied numerically for large enough system sizes and large enough statistics on the disordered samples to obtain accurate results, we have chosen to focus here on the power-law random banded matrices (PRBM) model, and to study numerically the statistical properties of the two-particle transmission T_2.

The paper is organized as follows. In section 2, we recall the PRBM model and introduce the observables that characterize transport properties for the two-particle model. In section 3, we describe our numerical results concerning the statistical properties of the transmission T_2 for two distinguishable particles, two bosons and two fermions. Our conclusions are summarized in section 4. In the appendix, we describe our numerical results concerning the multifractal properties of the one-particle model as a function of the energy E, which turn out to be useful to understand the statistics of T_2 discussed in the text.

2. Model and observables

2.1. Reminder on the power-law random banded matrices (PRBM) model

Besides the usual short-range Anderson tight-binding model in finite dimension d, other models displaying Anderson localization have been studied, in particular the PRBM model, which can be viewed as a one-dimensional model with long-ranged random hopping decaying as a power-law $(b/r)^a$ of the distance r with exponent a and parameter b. The Anderson transition at $a = 1$ between localized ($a > 1$) and extended ($a < 1$) states has been characterized in [27] via a mapping onto a nonlinear sigma model. The properties of the critical points at $a = 1$ have been studied considerably, in particular, the statistics of eigenvalues [28–30], and the multifractality of eigenfunctions [31–36], including boundary multifractality [37].

More precisely, we consider here the model shown in figure 1, with L sites $i = 1, 2, \ldots, L$ in a ring geometry with periodic boundary conditions. The appropriate distance $r_{i,j}$ between

the sites i and j is defined as [31]

$$r_{i,j}^{(L)} = \frac{L}{\pi} \sin\left(\frac{\pi(i-j)}{L}\right). \tag{1}$$

The ensemble of power-law random banded matrices of size $L \times L$ is then defined as follows: the matrix elements $H_{i,j}^{(1)}$ are independent Gaussian variables of zero-mean $\overline{H_{i,j}^{(1)}} = 0$ and of variance

$$\overline{\left(H_{i,j}^{(1)}\right)^2} = \frac{1}{1 + \left(\frac{r_{i,j}}{b}\right)^{2a}}. \tag{2}$$

The most important properties of this model are the following. The value of the exponent a determines the localization properties [27]: for $a > 1$ states are localized with integrable power-law tails, whereas for $a < 1$ states are delocalized. At criticality $a = 1$, states become multifractal [31–34] and exponents depend continuously on the parameter b, which plays a role analogous to the dimension d in short-range Anderson transitions [31]: the limit $b \gg 1$ corresponds to weak multifractality (analogous to the case $d = 2 + \epsilon$) and can be studied via the mapping onto a nonlinear sigma model [27], whereas the case $b \ll 1$ corresponds to strong multifractality (analogous to the case of high dimension d) and can be studied via Levitov renormalization [31, 38]. Other values of b have been studied numerically [31–34]. The statistical properties of the Landauer transmission for a single particle between the opposite points $L/2$ and L have been studied in detail in our previous work [39] (results concerning other scattering geometries can be found in [40]).

2.2. *Transmission of two distinguishable particles, two bosons or two fermions*

In this paper, we consider the two-particle model defined by the Hamiltonian

$$H^{(2)} = H^{(1)} \otimes 1 + 1 \otimes H^{(1)}. \tag{3}$$

As stressed in [15, 17, 19–21] for the one-dimensional TIP model, the important observation to characterize the two-particle transport properties is the Green's function

$$G_{E_2} \equiv \frac{1}{H^{(2)} - E_2} \tag{4}$$

between doubly occupied sites along the diagonal $r_1 = r_2$. In our present notations concerning the PRBM model (see figure 1), we will thus focus on the transmission

$$T_2 \equiv \left| \left\langle \frac{L}{2}, \frac{L}{2} \right| G_{E_2=0} |L, L\rangle \right|^2 \tag{5}$$

at zero energy $E_2 = 0$ (center of the band). It is important to stress that even if there is no explicit interaction in the Hamiltonian of equation (3), the two-particle Green's function cannot be factorized into one-particle properties [17, 20]. We will indeed find below non-trivial properties for T_2. As a comparison, one may also consider the transmission of one of the two particles with the other held fixed (see equation (7) of [19])

$$T_{2,(1f)} \equiv \left| \left\langle \frac{L}{2}, L \right| G |L, L\rangle \right|^2. \tag{6}$$

3. Numerical results on the statistical properties of T_2

3.1. Numerical procedure

We have used an exact diagonalization method, the one-particle PRBM model $H^{(1)}$, for the localization transition critical value $a = 1$ and for the parameter $b = 0.1$ (equation (2)). For each disordered sample, we note e_n the L eigenenergies ($n = 1, 2, \ldots, L$) and $\phi_n(i)$ the corresponding normalized eigenstates ($i = 1, 2, \ldots, L$)

$$H^{(1)}\phi_n(i) = e_n\phi_n(i). \tag{7}$$

To compute the two-particle Green's function, we now have to know the symmetry properties with respect to the exchange of the two particles.

3.1.1. Two distinguishable particles (no symmetry conditions). For two distinguishable particles, an orthonormal basis of eigenstates of $H^{(2)}$ is given by the following L^2 states labeled by two integers $1 \leqslant n \leqslant L$ and $1 \leqslant m \leqslant L$

$$\psi_{n,m}(i, j) = \phi_n(i)\phi_m(j) \tag{8}$$

of energy

$$E_{n,m} = e_n + e_m. \tag{9}$$

The two-particle Green's function at zero energy $E_2 = 0$ then reads

$$G_{E_2=0}(i, j; i', j') = -\sum_{n=1}^{L}\sum_{m=1}^{L}\frac{\psi^*_{n,m}(i, j)\psi_{n,m}(i', j')}{E_{n,m}} \tag{10}$$

$$= -\sum_{n=1}^{L}\sum_{m=1}^{L}\frac{\phi^*_n(i)\phi^*_m(j)\phi_n(i')\phi_m(j')}{e_n + e_m}. \tag{11}$$

3.1.2. Two bosons (symmetry condition). An orthonormal basis of eigenstates is given by the following $L(L+1)/2$ symmetric states labeled by two integers $1 \leqslant n \leqslant m \leqslant L$

$$\psi^B_{n,n}(i, j) = \phi_n(i)\phi_n(j) \tag{12}$$

$$\psi^B_{n,m}(i, j) = \frac{\phi_n(i)\phi_m(j) + \phi_m(i)\phi_n(j)}{\sqrt{2}} \tag{13}$$

of energy given by equation (9).

The two-boson Green's function at zero energy $E_2 = 0$ then reads

$$G^B_{E_2=0}(i, j; i'j') = -\sum_{n=1}^{L}\sum_{m=n}^{L}\frac{\psi^{B*}_{n,m}(i, j)\psi^B_{n,m}(i', j')}{e_n + e_m}. \tag{14}$$

3.1.3. Two fermions (antisymmetry condition). An orthonormal basis of eigenstates is given by the following $L(L-1)/2$ antisymmetric states labeled by two integers $1 \leqslant n < m \leqslant L$

$$\psi^F_{n,m}(i, j) = \frac{\phi_n(i)\phi_m(j) - \phi_m(i)\phi_n(j)}{\sqrt{2}} \tag{15}$$

of energy given by equation (9).

The two-fermion Green's function at zero energy $E_2 = 0$ then reads

$$G^F_{E_2=0}(i, j; i' j') = -\sum_{n=1}^{L-1} \sum_{m=n+1}^{L} \frac{\psi^{F*}_{n,m}(i, j)\psi^F_{n,m}(i', j')}{e_n + e_m}. \tag{16}$$

For fermions where double occupancy is forbidden, we have modified the definitions of equations (5) and (6) for the transmissions into

$$T_2^F \equiv |\langle L/2, L/2 - 1|G|L, L - 1\rangle|^2 \tag{17}$$

and

$$T^F_{2,(1f)} \equiv |\langle L/2 - 1, L|G|L - 1, L\rangle|^2. \tag{18}$$

The results given below correspond to sizes $50 \leqslant L \leqslant 2000$, with corresponding statistics of $5.10^7 \geqslant n_s(L) \geqslant 1150$ independent samples. To improve the statistics, we have considered, for each disordered sample, the transmission T_2 between the $L/2$ pairs of opposite points. All results concern the zero-energy ($E_2 = 0$) transmission T_2 at the critical point $a = 1$ and the value $b = 0.1$ (see equation (2)). We first focus on the scaling of the typical transmission before we turn to the multifractal spectrum.

3.2. *Typical transmission $T_2^{\rm typ}(L)$ as a function of L*

We find that the typical two-particle transmission

$$T_2^{\rm typ}(L) \equiv e^{\overline{\ln T_2(L)}} \tag{19}$$

decays as the power-law

$$T_2^{\rm typ}(L) \underset{L\to\infty}{\propto} \frac{1}{L^{\kappa_2^{\rm typ}}} \tag{20}$$

where

$$\kappa_2^{\rm typ} \simeq 1.86 \tag{21}$$

is the same for two distinguishable particles, two bosons or two fermions as shown in figure 2.

As a comparison, we also show in figure 2 the typical transmission $T^{\rm typ}_{2,(1f)}$ of equation (6) representing the transmission of one of the two particles with the other held fixed: for distinguishable particles, bosons or fermions, it is governed by the same exponent

$$\kappa^{\rm typ}_{2,(1f)} \simeq 1.3 \tag{22}$$

that coincides, within our error bars, with the exponent $\kappa_1^{\rm typ}$ measured in [39] for the one-particle model.

3.3. *Multifractal statistics of T_2*

We find that the statistics of T_2 is multifractal, i.e. that the probability to have $T_2(L) \sim 1/L^\kappa$ behaves as

$$\text{Prob}(T_2(L) \sim L^{-\kappa})\, dT \underset{L\to\infty}{\propto} L^{\Phi_2(\kappa)} d\kappa. \tag{23}$$

We show in figure 3 the multifractal spectra $\Phi_2(\kappa)$ corresponding to two distinguishable particles, two bosons and two fermions. We find that the spectra for distinguishable particles and bosons coincide, whereas the spectrum for fermions is clearly distinct, except around the maximum $\Phi_2\left(\kappa_2^{\rm typ}\right) = 0$ associated with the same typical value $\kappa_2^{\rm typ}$ of equation (21). This

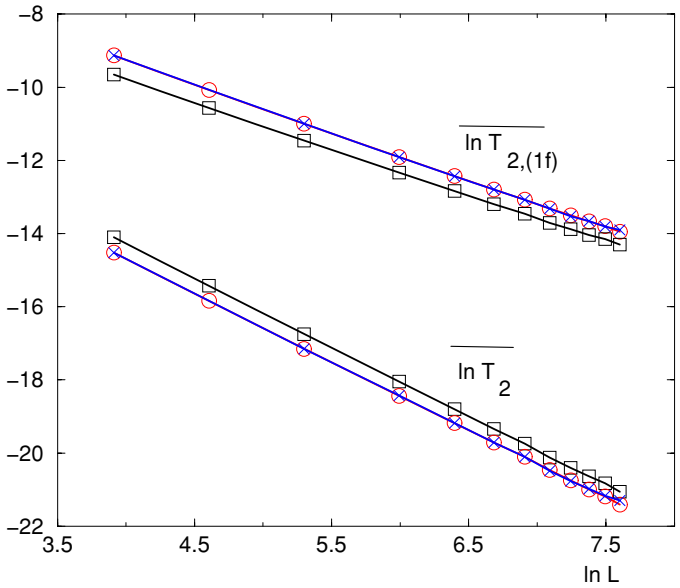

Figure 2. Scaling of the typical two-particle transmission $T_2^{\rm typ}$ at criticality $a = 1$ for $b = 0.1$ and at zero-energy $E = 0$: $\ln T_2^{\rm typ}(L) \equiv \overline{\ln T_2(L)}$ as a function of $\ln L$ for fermions (□), bosons (◯) and distinguishable particles (×) yield the same exponent $\kappa_2^{\rm typ} \simeq 1.86$ (equation (21)). As a comparison, the scaling of the typical transmission $T_{2,(1f)}^{\rm typ}$ of equation (6) (representing the transmission of one of the two particles with the other held fixed) corresponds to the exponent $\kappa_{2,(1f)}^{\rm typ} \simeq 1.3$ (equation (22)).

can be explained as follows: the transmission T_2 for distinguishable particles and bosons both involve coinciding points (equation (5)), whereas the transmission T_2 for fermions involves neighboring points (equation (17)). Besides their common typical scaling, one expects differences in their statistics, because in critical phenomena, the product of two neighboring fields has a non-trivial scaling dimension [42] (for instance in the Ising model, the local energy density which is the product of two neighboring spins has its own scaling dimension that cannot be obtained from the magnetization scaling dimension [42]).

As a comparison, we also show in figure 3 the multifractal spectrum $\Phi_1(\kappa)$ describing the statistics of the corresponding one-particle transmission T_1. A natural question is of course whether the multifractal spectrum $\Phi_2(\kappa)$ can be related to $\Phi_1(\kappa)$ or to the singularity spectrum of one-particle eigenfunctions.

3.4. Discussion: relation with the statistics of one-particle eigenfunctions

We first recall the case of the one-particle transmission, before we turn to the analysis of T_2.

3.4.1. Analysis of the one-particle transmission in terms of one-particle eigenfunctions. In terms of the energies e_n and eigenfunctions ϕ_n of the one-particle model (equation (7)), the one-particle zero-energy Green's function reads

$$g_{E_1=0}(i;i') = -\sum_{n=1}^{L} \frac{\phi_n^*(i)\phi_n(i')}{e_n}. \tag{24}$$

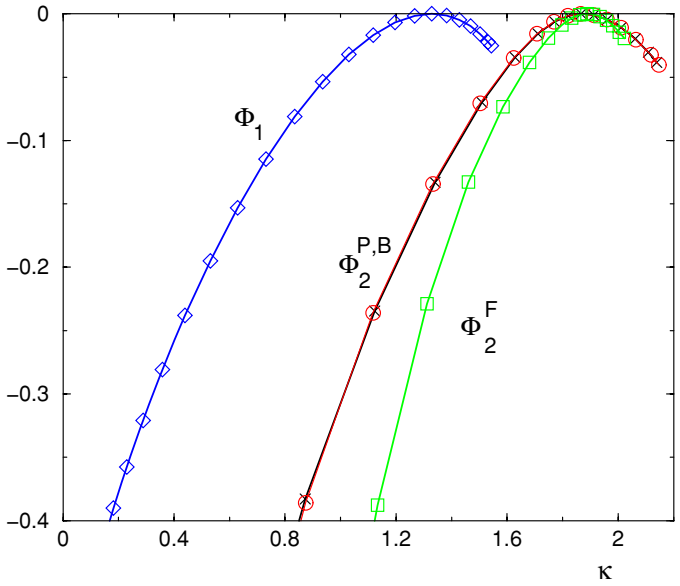

Figure 3. Multifractal spectra $\Phi_2(\kappa)$ describing the statistics of the transmission T_2 at criticality $a = 1$ for $b = 0.1$ and at zero-energy $E = 0$: for two fermions (□), two bosons (◯) and two distinguishable particles (×). As a comparison, the multifractal spectrum $\Phi_1(\kappa)$ describing the statistics of the corresponding one-particle transmission is shown (◇).

In the limit of large size L where the levels become dense, the zero-energy Green's function of equation (11) becomes

$$g_{E_1=0}(i;i') \sim -L^d \int \mathrm{d}e\, \rho(e) \frac{\phi_e^*(i)\phi_e(i')}{e} \tag{25}$$

which is dominated by the neighborhood of $e = 0$

$$g_{E_1=0}(i;i') \sim -L^d \phi_{e=0}^*(i)\phi_{e=0}(i') \tag{26}$$

so that the one-particle transmission scales as

$$T_1(i,i') = |g_{E_1=0}(i;i')|^2 \sim L^{2d} |\phi_{e=0}(i)|^2 |\phi_{e=0}(i')|^2. \tag{27}$$

When the distance $|i - i'|$ is of the order of the system size L, the weights $|\phi_{e=0}(i)|^2$ and $|\phi_{e=0}(i')|^2$ can be considered as independent. Then the multifractal spectrum $\Phi_1(\kappa)$ describing the distribution of the one-point transmission

$$\mathrm{Prob}\,(T_1 \sim L^{-\kappa})\,\mathrm{d}T \underset{L\to\infty}{\propto} L^{\Phi_1(\kappa)}\mathrm{d}\kappa \tag{28}$$

can be written as (here with $d = 1$)

$$\Phi_1(\kappa \geqslant 0) = 2\left[f\left(\alpha = d + \frac{\kappa}{2}\right) - d \right] \tag{29}$$

in terms of the singularity spectrum $f(\alpha)$ of zero-energy eigenfunctions (see more details in [39, 41]).

3.4.2. Analysis of the two-particle transmission in terms of one-particle eigenfunctions. We now try to analyze the two-point transmission T_2 for two distinguishable particles along the same lines. In the limit of large size L where the levels become dense, the zero-energy Green's function of equation (11) becomes

$$G_{E_2=0}(i,i;i',i') \sim -L^{2d} \int de\, \rho(e) \int de'\rho(e') \frac{\phi_e^*(i)\phi_{e'}^*(i)\phi_e(i')\phi_{e'}(i')}{e+e'} \quad (30)$$

which is dominated by the region $e + e' = 0$

$$G_{E_2=0}(i;i') \sim -L^{2d} \int de\, \rho^2(e)\phi_e^*(i)\phi_{-e}^*(i)\phi_e(i')\phi_{-e}(i') \quad (31)$$

(where we have used the symmetry $\rho(e) = \rho(-e)$ around the center of the band $e = 0$ for the one-particle density of states). The two-particle transmission is then expected to scale as

$$T_2(i,i') = |G_{E_2=0}(i;i')|^2 \sim L^{4d} \int de\, \rho^2(e) \int de'\rho^2(e')[\phi_e^*(i)\phi_{-e}^*(i)\phi_{e'}^*(i)\phi_{-e'}^*(i)] \times [\phi_e(i')\phi_{-e}(i')\phi_{e'}(i')\phi_{-e'}(i')]. \quad (32)$$

So we do not expect any simple expression for the multifractal spectrum $\Phi_2(\kappa)$: firstly, T_2 contains eigenfunctions of any energy e, and the singularity spectrum $f(\alpha)$ of one-particle eigenfunctions depends continuously on the energy e (see more details in the appendix); secondly, T_2 involves complicated correlations of eigenfunctions of various energies (studies of two-eigenfunctions correlations can be found in [43, 44]).

It is, however, natural to consider the simplest approximation: if the integrals in equation (32) were dominated by $e = 0 = e'$, one would obtain a direct relation with the one-particle transmission of equation (27)

$$T_2^{\text{approx}(a)}(i,i') \sim L^{4d}|\phi_{e=0}(i)|^4|\phi_{e=0}(i')|^4 \sim (T_1(i,i'))^2. \quad (33)$$

In particular, the typical exponent κ_2^{typ} would read

$$\kappa_2^{\text{typ}} = 2\kappa_1^{\text{typ}}. \quad (34)$$

Our numerical results described above (equations (21) and (22)) show that κ_2^{typ} is in fact much smaller than $(2\kappa_1^{\text{typ}})$. Our conclusion is thus that this simple approximation is very unsatisfactory, and that correlations between one-particle eigenfunctions at various energies play a major role in the two-particle transmission T_2.

4. Conclusion

In this paper, we have studied numerically the statistical properties of the two-particle transmission $T_2(L)$ in the non-interacting case, at the critical point of the PRBM model where one-particle eigenfunctions are known to be multifractal. Our conclusion is that $T_2(L)$ is multifractal i.e. the probability to have $T_2(L) \sim 1/L^\kappa$ behaves as $L^{\Phi_2(\kappa)}$, where the multifractal spectrum $\Phi_2(\kappa)$ for fermions is different from the common multifractal spectrum concerning distinguishable particles and bosons, because the double occupancy of a single site and the occupancy of two neighboring sites have different statistics at criticality. However, in the three cases, the typical transmission $T_2^{\text{typ}}(L)$ is governed by the same exponent κ_2^{typ}, which is much smaller than the naive expectation $2\kappa_1^{\text{typ}}$, where κ_1^{typ} is the typical exponent of the one-particle transmission $T_1(L)$. This suggests that $T_2(L)$ probes non-trivial correlations of one-particle eigenfunctions of various energies.

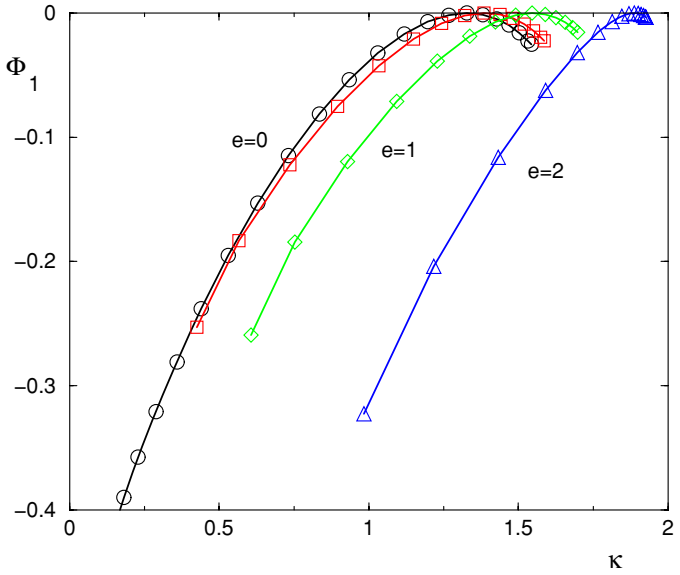

Figure 4. The multifractal spectrum $\Phi_1(\kappa)$ describing the statistics of the one-particle transmission (equation (28)) at criticality $a = 1$ and $b = 0.1$ for four values of the energy: $e = 0$ (◯), $e = 0.5$ (□), $e = 1$ (◇) and $e = 2$ (△).

Appendix. Multifractal statistics of the one-particle transmission as a function of energy

As first discussed in [41] for the special case of the two-dimensional quantum Hall transition, the critical probability distribution of the one-particle transmission T_1 at an Anderson transition critical point takes the form of equation (28) where the multifractal spectrum $\Phi_1(\kappa)$ can be related to the singularity spectrum $f(\alpha)$ of critical eigenstates via equation (29).

For the PRBM model, numerical results on $\Phi_1(\kappa)$ can be found in [39] at the critical point $a = 1$ and at zero energy $e = 0$ for various values of the parameter b (equation (2)).

Here we show in figure 4 how the multifractal spectrum $\Phi_1(\kappa)$ at criticality $a = 1$ for the value $b = 0.1$ changes as a function of the energy e. In particular, the corresponding typical values read

$$\begin{aligned} \kappa_1^{\rm typ}(e=0) &\simeq 1.33 \\ \kappa_1^{\rm typ}(e=0.5) &\simeq 1.38 \\ \kappa_1^{\rm typ}(e=1) &\simeq 1.55 \\ \kappa_1^{\rm typ}(e=2) &\simeq 1.89 \end{aligned} \tag{A.1}$$

Via equation (29), this shows that the singularity spectrum $f(\alpha)$ of critical eigenfunctions changes with the energy e. (The dependence on e of $f(\alpha)$ has been studied in [45] for quantum Hall wavefunctions as a function of the Landau level.)

Since the zero-energy two-particle transmission T_2 of equation (32) contains one-particle eigenfunctions of various energies, that are characterized by different multifractal singularity spectra, we do not expect any simple expression for the multifractal spectrum $\Phi_2(\kappa)$ of T_2.

References

[1] Anderson P W 1958 *Phys. Rev.* **109** 1492
[2] Janssen M 1998 *Phys. Rep.* **295** 1
[3] Markos P 2006 *Acta Phys. Slovaca* **56** 561
[4] Evers F and Mirlin A D 2008 *Rev. Mod. Phys.* **80** 1355
[5] Belitz D and Kirkpatrick T R 1994 *Rev. Mod. Phys.* **66** 261
[6] Basko D M, Aleiner I L and Altshuler B L 2006 *Ann. Phys.* **321** 1126
Basko D M, Aleiner I L and Altshuler B L 2007 *Phys. Rev.* B **76** 052203
[7] Altshuler B L, Gefen Y, Kamenev A and Levitov L S 1997 *Phys. Rev. Lett.* **78** 2803
[8] Silvestrov P G 2001 *Phys. Rev.* B **64** 113309
[9] Gornyi I V, Mirlin A D and Polyakov D G 2005 *Phys. Rev. Lett.* **95** 206603
[10] Oganesyan V and Huse D A 2007 *Phys. Rev.* B **75** 155111
[11] Fleury G and Waintal X 2008 *Phys. Rev. Lett.* **100** 076602
Fleury G and Waintal X 2008 *Phys. Rev. Lett.* **101** 226803
[12] Dorokhov O N 1990 *Zh. Eksp. Teor. Fiz.* **98** 646
Dorokhov O N 1990 *Sov. Phys.-JETP* **71** 360
[13] Shepelyansky D L 1994 *Phys. Rev. Lett.* **73** 2607
[14] Weinmann D and Pichard J L 1996 *Phys. Rev. Lett.* **77** 1556
[15] von Oppen F, Wettig T and Müller J 1996 *Phys. Rev. Lett.* **76** 491
[16] Ponomarev I V and Silvestrov P G 1997 *Phys. Rev.* B **56** 3742
[17] Song P H and Kim D 1997 *Phys. Rev.* B **56** 12217
[18] Waintal X and Pichard J L 1998 *Eur. Phys. J.* B **6** 117
Waintal X, Weinmann D and Pichard J L 1999 *Eur. Phys. J.* B **7** 451
[19] Song P H and von Oppen F 1999 *Phys. Rev.* B **59** 46
[20] Leadbeater M, Römer R A and Schreiber M 1999 *Eur. Phys. J.* B **8** 643
[21] Römer R A, Leadbeater M and Schreiber M 1999 *Ann. Phys. (Leipzig)* **8** 5
Römer R A, Schreiber M and Vojta T 2001 *Physica* E **9** 397
[22] Ortuno M and Cuevas E 1999 *Euro. Phys. Lett.* **46** 224
[23] Cuevas E 1999 *Phys. Rev. Lett.* **83** 140
[24] Shepelyansky D L 2000 *Phys. Rev.* B **61** 4588
Benenti G and Shepelyansky D L 2001 *Phys. Rev.* B **63** 235103
[25] Talamantes J and Pollak M 2000 *Phys. Rev.* B **62** 12785
[26] Eilmes A, Grimm U, Römer R A and Schreiber M 1999 *Eur. Phys. J.* B **8** 547
Schuster C, Römer R A and Schreiber M 2002 *Phys. Rev.* B **65** 114114
[27] Mirlin A D *et al* 1996 *Phys. Rev.* E **54** 3221
[28] Varga I and Braun D 2000 *Phys. Rev.* B **61** R11859
[29] Kravtsov V E *et al* 2006 *J. Phys. A: Math. Gen.* **39** 2021
[30] Garcia-Garcia A M 2006 *Phys. Rev.* E **73** 026213
[31] Evers F and Mirlin A D 2000 *Phys. Rev. Lett.* **84** 3690
Mirlin A D and Evers F 2000 *Phys. Rev.* B **62** 7920
[32] Cuevas E, Gasparian V and Ortuno M 2001 *Phys. Rev. Lett.* **87** 056601
[33] Cuevas E *et al* 2002 *Phys. Rev. Lett.* **88** 016401
[34] Varga I 2002 *Phys. Rev.* B **66** 094201
[35] Cuevas E 2003 *Phys. Rev.* B **68** 024206
[36] Mirlin A D *et al* 2006 *Phys. Rev. Lett.* **97** 046803
[37] Mildenberger A *et al* 2007 *Phys. Rev.* B **75** 094204
[38] Levitov L S 1989 *Europhys. Lett.* **9** 83
Levitov L S 1990 *Phys. Rev. Lett.* **64** 547
Altshuler B L and Levitov L S 1997 *Phys. Rep.* **288** 487
Levitov L S 1999 *Ann. Phys. (Leipzig)* **8** 507 5
[39] Monthus C and Garel T 2009 *Phys. Rev.* B **79** 205120
[40] Monthus C and Garel T 2009 *J. Stat. Mech.* P07033
[41] Janssen M, Metzler M and Zirnbauer M R 1999 *Phys. Rev.* B **59** 15836
[42] Cardy J 1996 *Scaling and Renormalization in Statistical Physics* (Cambridge: Cambridge University Press)
[43] Fyodorov Y V and Mirlin A D 1997 *Phys. Rev.* B **55** R16001
[44] Cuevas E and Kravtsov V E 2007 *Phys. Rev.* B **76** 235119
[45] Terao T, Nakayama T and Aoki H 1996 *Phys. Rev.* B **54** 10350